Defective Temporal and Spatial Control of Flagellar Assembly in a Mutant of *Chlamydomonas reinhardtii* with Variable Flagellar Number

G. MIKE W. ADAMS, ROBIN L. WRIGHT,* and JONATHAN W. JARVIK*
*Department of Botan, Louisiana State University, Baton Rouge, Louisiana 70803; and *Department of Biological Sciences, Carnegie-Mellon University, Pittsburgh, Pennsylvania 15213*

ABSTRACT Wild-type *Chlamydomonas reinhardtii* carry two flagella per cell that are used for both motility and mating. We describe a mutant, *vfl-1*, in which the biflagellate state is disrupted such that the number of flagella per cell ranges from 0 to as many as 10. *vfl-1* cells possess the novel ability to assemble new flagella throughout the G_1 portion of the cell cycle, resulting in an average increase of about 0.05 flagella per cell per hour. Such uncoupling of the flagellar assembly cycle from the cell cycle is not observed in other mutants with abnormal flagellar number. Rather than being located in an exclusively apical position characteristic of the wild type, *vfl-1* flagella can be at virtually any location on the cell surface. *vfl-1* cells display abnormally wide variations in cell size, probably owing to extremely unequal cell divisions. Various ultrastructural abnormalities in the flagellar apparatus are also present, including missing or defective striated fibers and reduced numbers of rootlet microtubules. The pleiotropic defects observed in *vfl-1* result from a recessive Mendelian mutation mapped to Chromosome VIII.

The basal body developmental cycle of the unicellular biflagellate green alga, *Chlamydomonas reinhardtii*, represents a clear case in which organelle replication is coupled to cell replication. In the basal body cycle, new basal bodies form at determined times and places during interphase, and they segregate equally at cell division to yield biflagellate daughter cells (2, 8). Through the analysis of mutants with defects in the basal body cycle, we hope to gain insight into the mechanisms of basal body biogenesis and segregation, and also into the mechanisms by which cell and organelle cycles are coordinated. In this communication we describe a mutant, *vfl-1*, in which the temporal and spatial regulation of the basal body cycle is defective. As a result, *vfl-1* cells have the novel property of assembling new flagella continuously throughout much of the cell cycle.

MATERIALS AND METHODS

Strains and Culture Conditions: *vfl-1* was derived from the strain CC-70 *mt*⁻ (Chlamydomonas Culture Collection, Duke University) in a general screening for motility-defective mutants following mutagenesis with *N*-methyl-*N'*-nitro-*N*-nitrosoguanidine (1). Cells were grown at 25°C in medium I of Sager and Granick (14). Synchronization was achieved by a 14-h light/10-h dark illumination schedule unless otherwise specified.

Measurement of Flagellar Number, Length, and Location: Cells were fixed by the addition of ½ vol of 1% aqueous glutaraldehyde and examined at ×800 using phase-contrast optics for determination of flagellar number and location. Flagellar length was measured with an ocular micrometer using phase-contrast or Nomarski differential interference contrast optics. Distributions of flagellar number and location were based on samples of at least 200 cells and flagellar length averages were based on samples of at least 20 cells per flagellar number class. Cell volumes were determined by measuring cell length and width and applying the equation $\pi/6 \times (\text{width})^2 \times \text{length}$ (13).

Determination of Flagellar Number Changes in Living Cells and Mitotic Pedigree Analysis: Cells in the first hour of the light segment of the cycle were suspended in 0.5% melted agar. A drop was placed within a ring of petroleum jelly on a slide and sealed with a coverslip. Approximately 1 h later, cell positions were determined using the microscope stage's vernier scales, and cell size, flagellar number, and flagellar lengths were recorded. The slides were maintained at standard illumination for an additional 5 h and the cells were observed again. They were then returned to standard illumination conditions overnight, during which one or more rounds of mitosis per cell division typically took place. The next morning the number and size of daughter cells were measured along with the number of flagella on each cell.

THE JOURNAL OF CELL BIOLOGY · VOLUME 100 MARCH 1985 955-964

Genetic Analysis: Standard techniques were used for crosses and tetrad dissections (6, 9). Mapping stocks were those listed in Adams et al. (1). Dominance was assessed in *arg-2/arg-7, vfl-1/vfl-1*$^+$ diploids (5).

Electron Microscopy: Log-phase cells between the second and fourth hour of the light segment of the illumination cycle were harvested by centrifugation (5 min at 2,500 rpm). The pellet was resuspended in residual culture medium and 2 ml freshly prepared fixative (2.5% glutaraldehyde, 2% osmium tetroxide in 0.1 M sodium cacodylate buffer, pH 7.8) was added (7). After 5 min on ice the cells were repelleted and the initial fixative was replaced with an equal volume of fresh fixative. After 30 min the cells were washed at least five times with 0.1 M sodium cacodylate buffer and stored overnight at 4°C. Pellets were postfixed for 2 h in 2% osmium tetroxide in 0.1 M cacodylate and then rinsed twice with water. If en bloc staining was to be performed, the cells were given an additional two washes with 50% aqueous ethanol. En bloc staining was accomplished with 0.25–0.5% aqueous uranyl acetate for 15 min or, for cases in which enhanced microtubule contrast was desired, 4% tannic acid in 0.1 M sodium cacodylate.

Samples were rapidly dehydrated in a graded alcohol series, rinsed twice in propylene oxide, and infiltrated with resin (60 ml dodececenyl succinic anhydride, 20 ml Araldite 502, 20 ml Embed 812, 3 ml 2,4,6-tri(dimethylaminomethyl)phenol-30); Electron Microscopy Sciences, Fort Washington, PA). Infiltration was facilitated by use of a vacuum oven (50°C, 10 psi) and the resin was polymerized at the same setting for 12–24 h. Silver to gold sections were cut using a diamond knife on a Sorvall MT-1 microtome (DuPont Instruments—Sorvall Biomedical Div., DuPont Co., Wilmington, DE). Sections were stained with 3% aqueous uranyl acetate and Reynold's lead citrate and examined with a Phillips 300 electron microscope at 60kV.

RESULTS

Flagellar Number, Location, and Motility in vfl-1

vfl-1 was isolated after nitrosoguanidine mutagenesis of wild-type *C. reinhardtii* (1). Most mutant cells carry from zero to four flagella each, but rare cells can have as many as 10. Fig. 1 shows the distribution of flagellar number classes in a typical *vfl-1* culture, and Fig. 2 shows differential interference contrast micrographs of a number of *vfl-1* cells. In some cells the flagella are paired as in wild type (Fig. 2, *B* and *G*) but in others they clearly are not (Fig. 2, *C*, D, and *H*). Flagella can be anywhere on the *vfl-1* surface, in marked contrast to wild type in which the flagella are always at the anterior cell apex. However, on multi-flagellated cells the flagella are usually clustered in the same general area.

Motility in *vfl-1* is severely impaired, even for those cells carrying two flagella. Many cells spin in place; others tumble wildly through the medium. Fewer than 1% of cells show a motility pattern that could be confused with that of wild type. Since ~20% of *vfl-1* cells are typically biflagellate, this means that even biflagellate cells swim aberrantly.

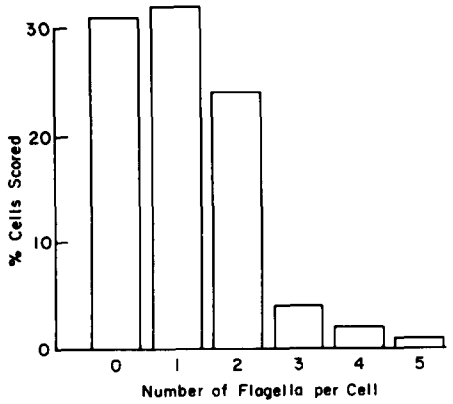

FIGURE 1 Distribution of flagella on synchronous early G_1 *vfl-1* vegetative cells. 440 cells were scored.

Cell Morphology and Growth

vfl-1 cells show extreme variation in size and are often abnormal in shape. Measured cell volumes for 100 mid-G_1 *vfl-1* cells ranged from 24 to 1423 μm^3, whereas wild-type controls ranged from 72 to 733 μm^3. The range in size seen in these controls is typical of rapidly growing light/dark–synchronized *Chlamydomonas* cultures, in which many cells undergo two or more rounds of mitosis during the dark portion of the cycle (4). No obvious correlation was seen between cell size and flagellar number (Fig. 3*A*), but, as in wild type, cells with larger volumes tended to have somewhat longer flagella (Fig. 3*B*).

Microscopic observation of microcolonies derived from

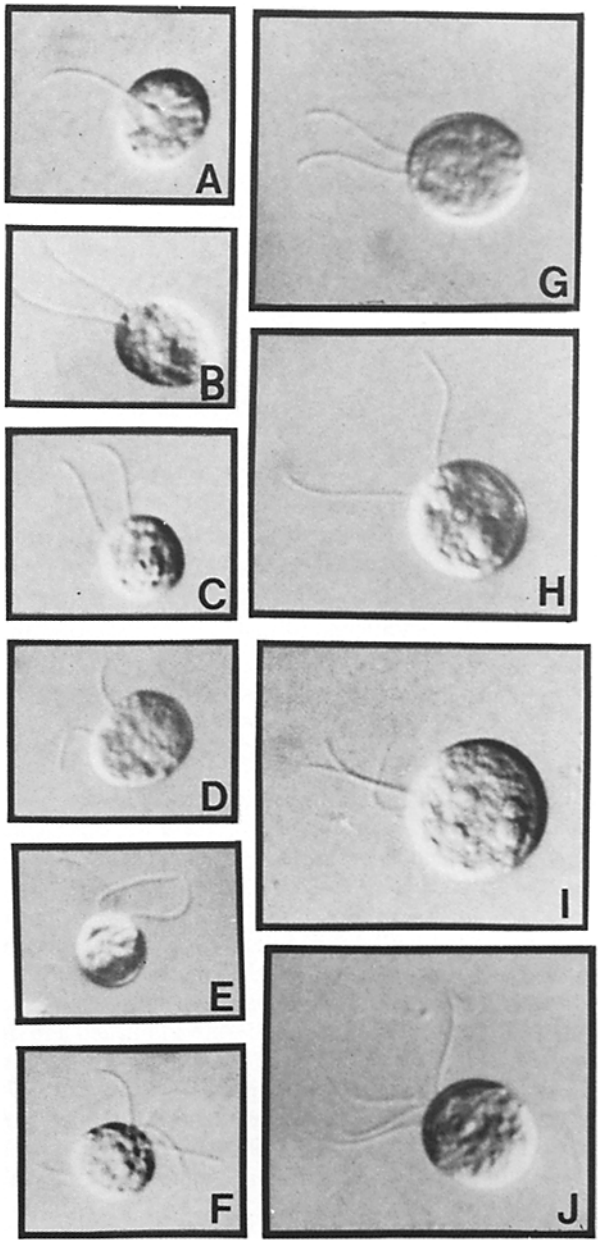

FIGURE 2 Nomarski differential interference contrast micrographs of glutaraldehyde-fixed *vfl-1* vegetative cells (× 3,400). Note wide variations in cell size and in the number and location of flagella. The cell in *B* closely resembles wild type in size and flagellar placement.

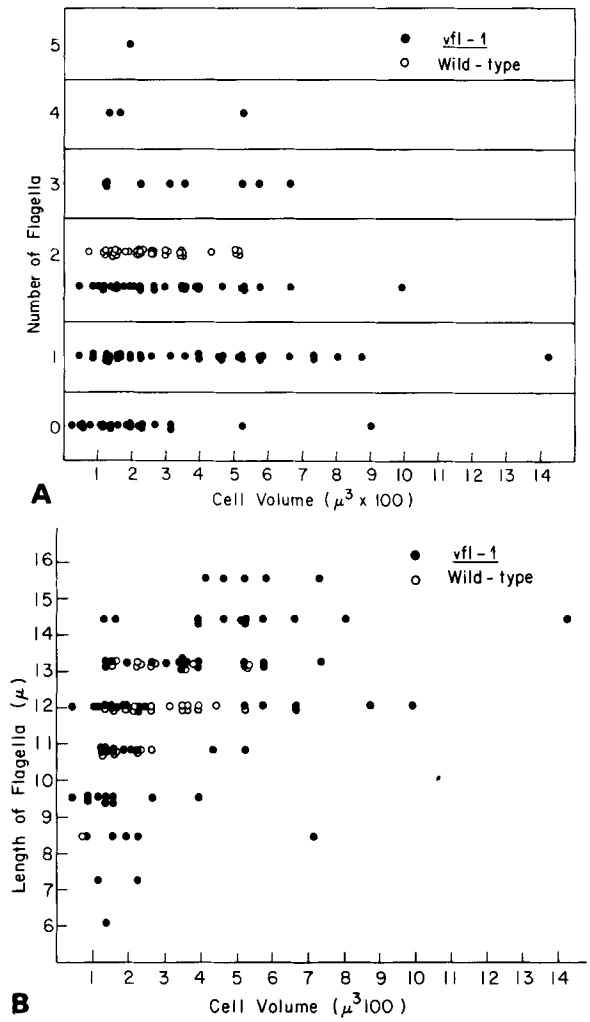

FIGURE 3 (*A*) Relationship between cell volume and number of flagella in *vfl-1* and wild type. Note the broad size variation in *vfl-1* cells regardless of flagellar numbers. Note also the lack of any simple correlation between the number of flagella and the size of the cell. (*B*) Relationship between cell volume and flagellar length in *vfl-1* and wild type. Note that although there is a general trend in both strains for larger cells to carry longer flagella, there are many cases in which large cells carry short flagella or small cells carry long flagella.

single agar-immobilized cells indicated frequent segregation of inviable progeny at cell division. Extremely unequal divisions were common, producing inviable daughter cells as small as 1 μm diam. Counts of cell number in day-old microcolonies gave values of from 2 to 23 cells per colony for *vfl-1*, whereas wild-type control colonies were much more uniform, containing between two and eight cells in almost every case (Fig. 4). Note that nearly all wild-type colonies contained an even number of cells, whereas a great many *vfl-1* colonies contained an odd number, consistent with the death of some mitotic progeny or the failure of some daughters to divide again. 17% of the mutant cells had not divided at all and of these 6% were clearly dead.

vfl-1 Cells Acquire New Flagella throughout G1

A number of results demonstrate clearly that *vfl-1* cells acquire new flagella throughout the G_1 phase of the cell cycle. In one experiment, a synchronous culture growing on a 12-h light/dark regime was sampled at intervals and the mean number of flagella per cell was determined. As indicated in Fig. 5, the number was lowest immediately after cell division and showed a linear increase throughout G_1 (i.e., throughout the light period of the cell cycle) at a rate of 0.056 per cell per hour.

In another experiment, single cells of synchronized *vfl-1* culture were immobilized in agar and the number of flagella on individual cells was recorded 1 and 6 h later. As the results presented in Table I indicate, cells of all flagellar number classes could add new flagella in G_1. When the data are considered together, they give an average flagellar number per cell of 1.26 at the time of the initial observation, and a value of 1.51 5 h later. This represents a rate of 0.05 flagella per cell per hour, a value very close to the 0.056 rate derived independently as described above. In control experiments using wild-type or *vfl-3* cells (17), no increase in flagellar number during G_1 was observed. Table II*A* demonstrates that the initial distribution of flagella among individual *vfl-1* cells was random or very nearly so, since the flagella-number classes

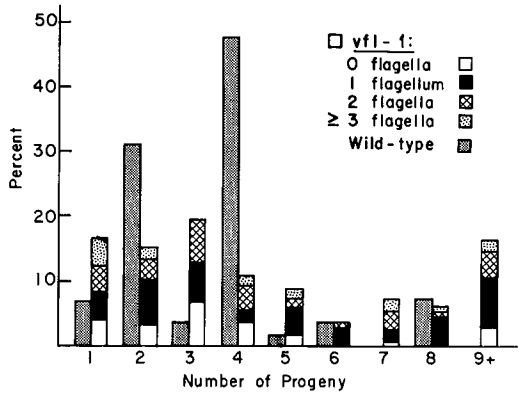

FIGURE 4 Composition of microcolonies derived from the division of single cells. The overall percentage of observed microcolonies with 1, 2, 3 (etc) cells is depicted by the height of the bars. (Wild-type results are closely stippled.) *vfl-1* results are divided according to the flagellar number of the parental cells. For example, the rightmost bar shows that 18% of the *vfl-1* parental cells divided to produce microcolonies containing nine daughter cells. The solid portion of this bar shows that 48% of these parental cells carried one flagellum before division. Note the wide variation in number of progeny produced by *vfl-1* parent cells and that parental flagellar number appears unrelated to the number of daughter cells produced during one round of division. Sample sizes were: *vfl-1*, 125 cells; wild type, 64 cells.

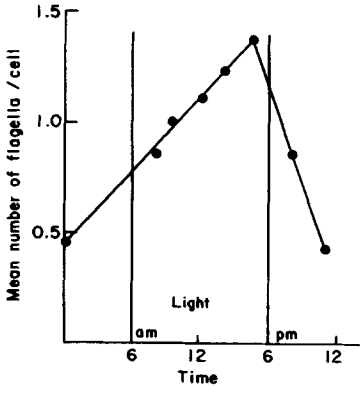

FIGURE 5 Mean number of flagella per cell in *vfl-1* culture throughout the cell cycle. *vfl-1* cells were grown on a 12-h light, 12-h dark cycle; the cells divided between midnight and 3 a.m. Sample size was between 400 and 600 cells at each time point. The least squares regression line for the points between midnight and the end of the light cycle has a slope of 0.056 flagella per cell per h ($r = 0.995$).

closely fit a Poisson distribution. Furthermore, the addition of new flagella during the 5-h interval was random (Table IIb).

Flagellar number was also observed for individual agar-immobilized *vfl-1* cells before and again after cell division. The results, summarized in Table III, indicated a tendency for cells with few flagella to yield progeny with few, and for cells with many flagella to yield progeny with many. This is not surprising because basal bodies persist through cell division and presumably can nucleate new flagella in the next generation. Consistent with these results was the observation that small clones (approximately 2,000 cells each) varied widely in terms of average flagellar number per cell (Table IV). Nonetheless, flagellar distributions within individual clones were random (i.e., closely fit Poisson distributions) irrespective of average flagellar number.

vfl-1 Ultrastructure

ORGANELLE PLACEMENT DEFECTS: As Fig. 6 illustrates, the geometrical relationships among the major cell organelles were frequently observed to be aberrant in *vfl-1*. In Fig. 6*A*, the normal positioning of the flagellar apparatus, nucleus, chloroplast, and pyrenoid in a wild-type cell is evident. Note the abnormality of flagellar position on the *vfl-1* cell in Fig. 6*B*: the flagellum appears on the side of the cell, with a lobe of the chloroplast passing between the basal body and the nucleus, a situation never observed in wild-type sections. The *vfl-1* cell membrane was often thrown into deep folds, especially at the anterior end of the cell (Fig. 6*C*). Chloroplasts appeared somewhat irregular in shape relative to the cup-shaped chloroplasts of wild type, and eyespots often displayed abnormal morphology or were present in multiple

TABLE I

Addition of Flagella to Individual vfl-1 Cells

Flagella per cell		Change in flagella number	Occurrences
Initial	After 5 h		
No.			*No.*
0	0	—	48
0	1	+1	4
0	2	+2	6
0	4	+4	1
1	1	—	68
1	2	+1	14
1	3	+2	3
1	4	+3	1
2	2	—	56
2	3	+1	11
2	5	+3	1
3	3	—	15
3	4	+1	2
4	4	—	3
5	5	—	1
6	7	+1	1

TABLE II

Distribution of Initial Flagellar Number Classes and of Flagella Added to Cells in 5 h

	Flagella/cell						
A	0	1	2	3	4	5	6
Observed	25.1	36.6	28.9	7.2	1.3	0.4	0.4
Poisson	28.5	35.7	22.5	9.5	3.0	0.7	0.1

	Flagella added per cell				
B	0	1	2	3	4
Observed	81.3	13.6	3.8	0.8	0.4
Poisson	77.8	19.5	2.5	0.2	0.01

For initial cell population distribution (*A*), $M = 1.26$, and for flagella added population (*B*), $M = 0.25$. $n = 235$ cells. Frequencies are expressed as percentages.

TABLE III

Flagella Number for Parent and Daughter vfl-1 Cells

Parent cells		Daughter cells	
Flagella number	Number of cells	Average number of flagella	Number of cells
0	21	0.73	80
1	41	1.0	178
2	23	1.2	79
3	9	1.2	31
>3	5	2.1	10

TABLE IV

Flagella Number Distributions in Small vfl-1 Clones

	Flagella per cell								
	0	1	2	3	4	5	6	*M*	Sample size
Observed	89.2	8.5	2.3	—	—	—	—	0.13	400
Poisson	87.8	11.4	0.9	—	—	—	—		
Observed	70.7	27.3	2.0	—	—	—	—	0.31	300
Poisson	73.3	22.7	3.5	—	—	—	—		
Observed	35.8	37.4	19.0	5.8	2.0	—	—	1.01	500
Poisson	36.5	36.8	18.5	6.2	1.5	—	—		
Observed	25.0	34.0	27.5	8.5	3.0	1.0	1.0	1.38	200
Poisson	25.3	34.8	23.9	11.0	3.8	1.0	0.2		
Observed	20.3	30.0	28.3	15.7	4.7	0.0	1.0	1.59	300
Poisson	20.5	32.5	25.7	13.6	5.4	1.7	0.5		

Five clones of approximately 2,500 cells each were chosen so that a wide range in the mean number of flagella per cell was represented. Frequencies are expressed as percentages. A minus (—) indicates that both the observed and calculated values were <0.1%.

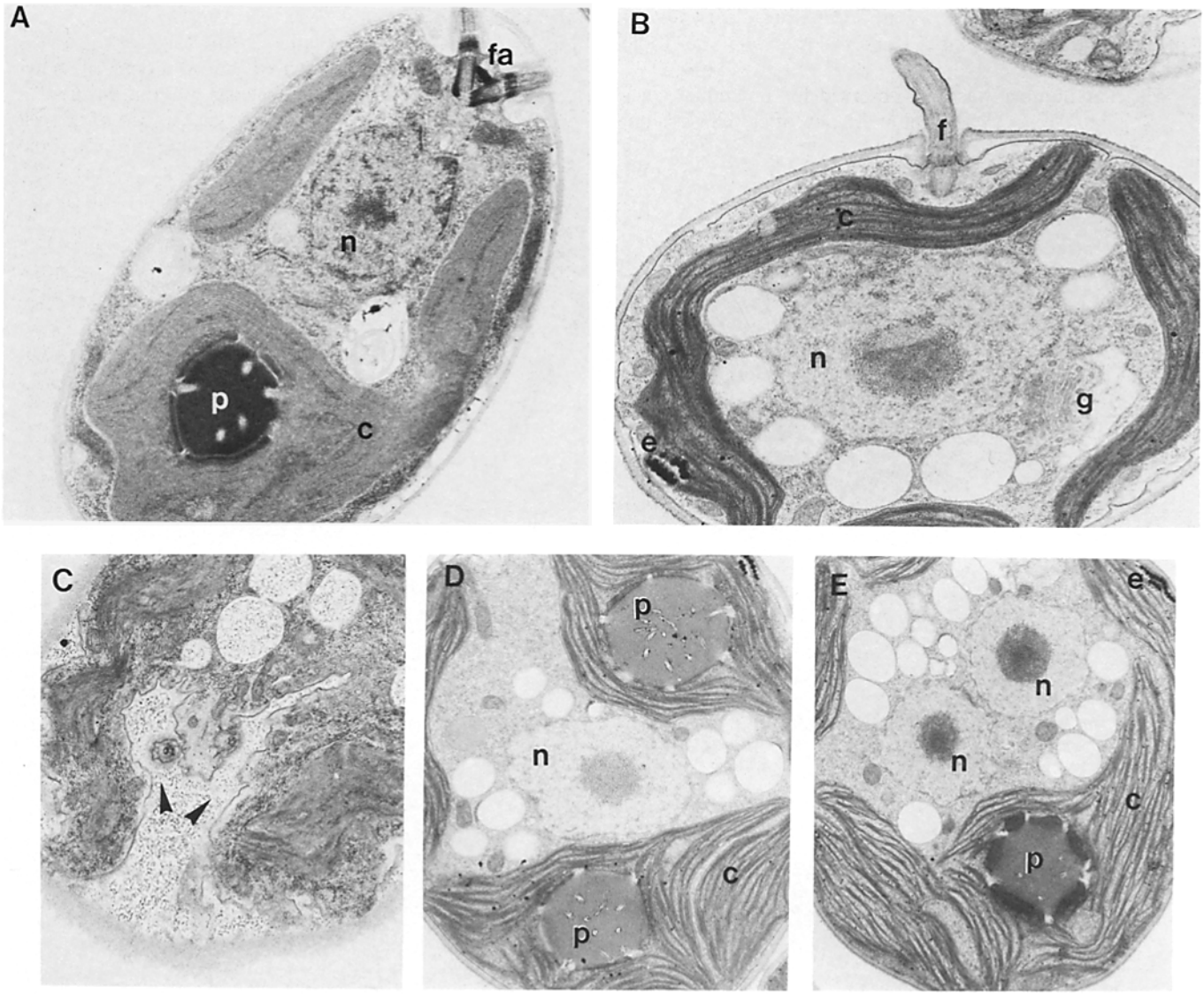

FIGURE 6 Cell shape and organelle position/number abnormalities in *vfl-1*. (*A*) Wild-type cells have a centrally located nucleus, a cup-shaped chloroplast containing a pyrenoid, and an anterior flagellar apparatus consisting of two flagella, two basal bodies, one distal and two proximal striated fibers, and a cruciate system of four microtubular rootlets (not all visible in this section). The long axis of the cell is anterior/posterior, with the flagella at the anterior apex and the pyrenoid at the posterior. × 13,500. (*B*) The flagellum is abnormally positioned on this *vfl-1* cell: it is located on the side (i.e., on the short axis) of the cell. Note the chloroplast lobe that passes between the basal bodies and nucleus, an arrangement never observed in wild type. × 13,500 (C) *vfl-1* cells often display deep invaginations in the cell membrane. In such cells, one or more basal bodies can be found in the center of the depression and the cell wall retains its normal ovoid shape. × 10,650. Multiple organelles are occasionally observed in *vfl-1* cells: (*D*) Two pyrenoids. × 9,000. (*E*) Two nuclei. × 7,350. *c*, chloroplast; *e*, eyespot; *fa*, flagellar apparatus; *g*, Golgi body; *n*, nucleus; *p*, pyrenoid.

locations in the chloroplast. Binucleate and/or bipyrenoidal cells were fairly common (Fig. 6, *D* and *E*). Golgi apparatuses were prominent, with as many as five appearing in a single section through a cell, and cells were generally highly vacuolated.

Aberrent morphology was especially apparent in sections through "palmelloid clusters" in which several daughter cells were retained within a mother wall. In such cases nuclei were often found very close to the plasma membrane rather than in the normal cytocentric location.

BASAL BODY, STRIATED FIBER, AND CYTOSKELETON DEFECTS: Most *vfl-1* basal bodies appeared normal in ultrastructure, but their positions in the cell and their orientations with respect to each other and to other cellular organelles were highly variable and rarely normal (Fig. 7). Basal bodies were sometimes found in the cell interior, either oriented parallel to the cell surface (Fig. 7*A*) or inverted, with the transition region, if present, pointing inward (Fig. 7, *B* and *C*). In several instances a basal body bearing an axoneme was observed deep within the cell (Fig. 7*D*). These axonemes were always membrane bounded, so that they resembled the primary cilia which have been observed in cultured animal cells (16). Many basal bodies at the cell surface carried no axonemes at all, terminating instead just above the transition region (Fig. 8 *D*). In some instances tunnels were present in the cell wall overlying the basal bodies, but in other instances no tunnels (Fig. 8*C*) were apparent. Other basal bodies at the cell surface appeared to carry only very short axonemes.

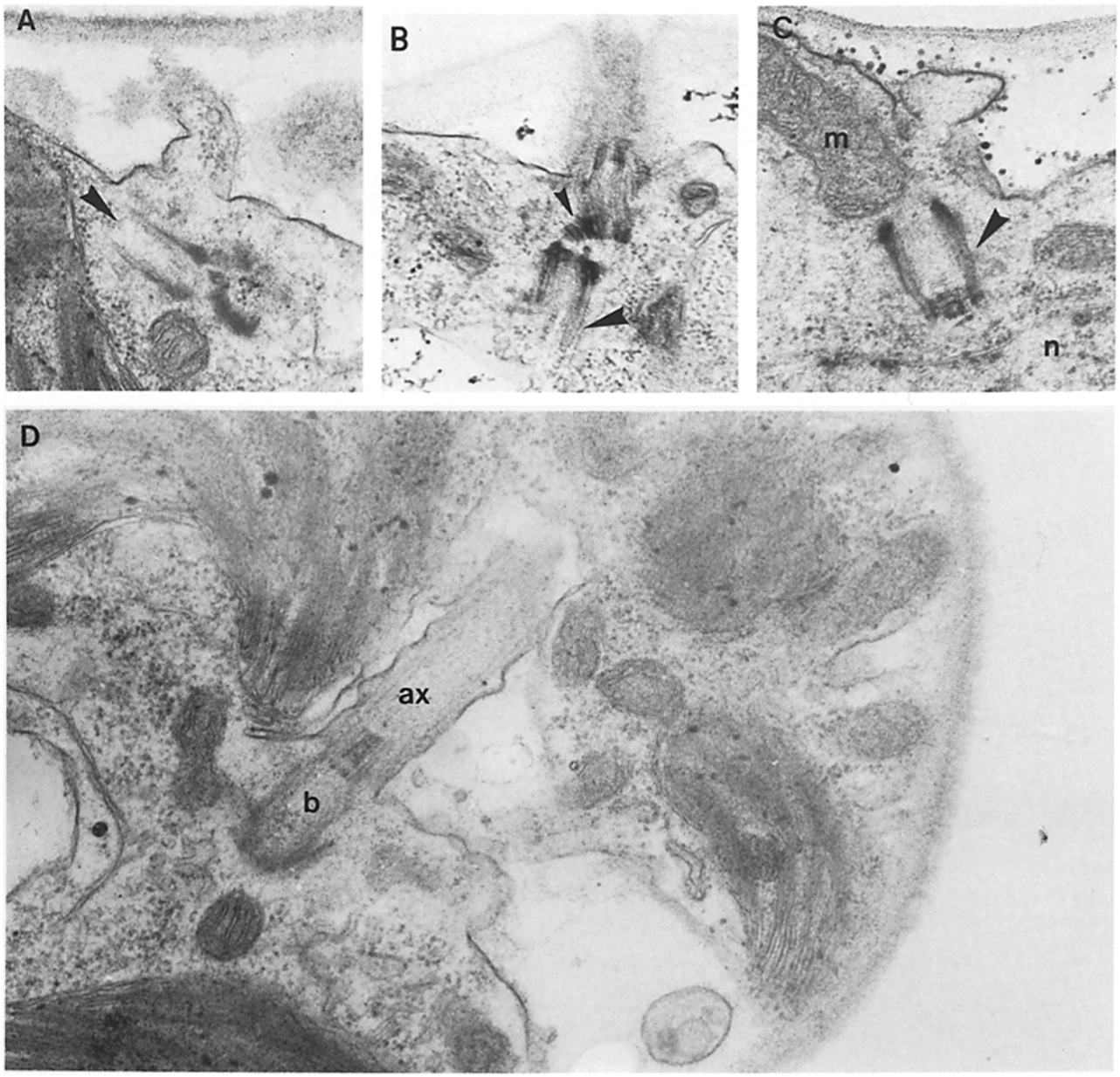

FIGURE 7 Variable basal body positioning and orientation in *vfl-1*. (*A*) The longitudinally sectioned basal body (large arrow) is oriented parallel, rather than perpendicular, to the cell membrane. Note absence of a transition region on the basal body and lack of an overlying tunnel through the cell wall. The membrane abnormalities seen here (blebs of cytoplasm above the basal body) are not uncommon. × 34,100. (*B*) The axes of the basal bodies in this section are oriented at ~180°. The upper one is in a normal orientation with respect to the cell and lies beneath a tunnel. The lower basal body (large arrow) points toward the cell interior. Note the presence of what appears to be a proximal striated fiber on the upper basal body (small arrow). × 43,900. (*C*) A well-defined basal body is positioned with its transition region toward the nucleus. It is extremely rare to observe transition regions on nonflagellated basal bodies. (*D*) An example of a membrane-bounded axoneme occurring deep in the cytoplasm. The plasma membrane is deeply folded and continuous with the flagellar membrane. Such structures have been observed in longitudinal sections such as this as well as in cross section. × 41,100. *ax*, axoneme; *b*, basal body; *m*, mitochondrion; *n*, nucleus.

Electron-dense rings of approximate basal body diameter were frequently observed in the cytoplasm of *vfl-1* cells (Fig. 8, *A* and *B*); such rings were not observed in wild type or in *vfl-3*, another variable flagella mutant whose ultrastructure was closely examined (17). Occasional basal bodies with doublet rather than triplet microtubules were also seen in *vfl-1* (Fig. 8 *E*) but not in *vfl-3* or wild type controls. We suspect that the rings and doublet basal bodies represent intermediates in basal body assembly (see Discussion).

Basal body–associated striated fibers were absent, incomplete, or misoriented in *vfl-1*. The position and ultrastructure of striated fiber connections in wild-type cells are depicted in Fig. 9, *A* and *B*. The striated fiber abnormalities observed in *vfl-1* include the apparent absence of the distal fiber (Fig. 9 *C*) and the presence of abnormal projections from basal bodies at a level where a distal fiber should normally appear (Fig. 9, *D*, *E*, and *F*). Both electron-dense and striated projections were observed. In an occasional case, an intact distal fiber

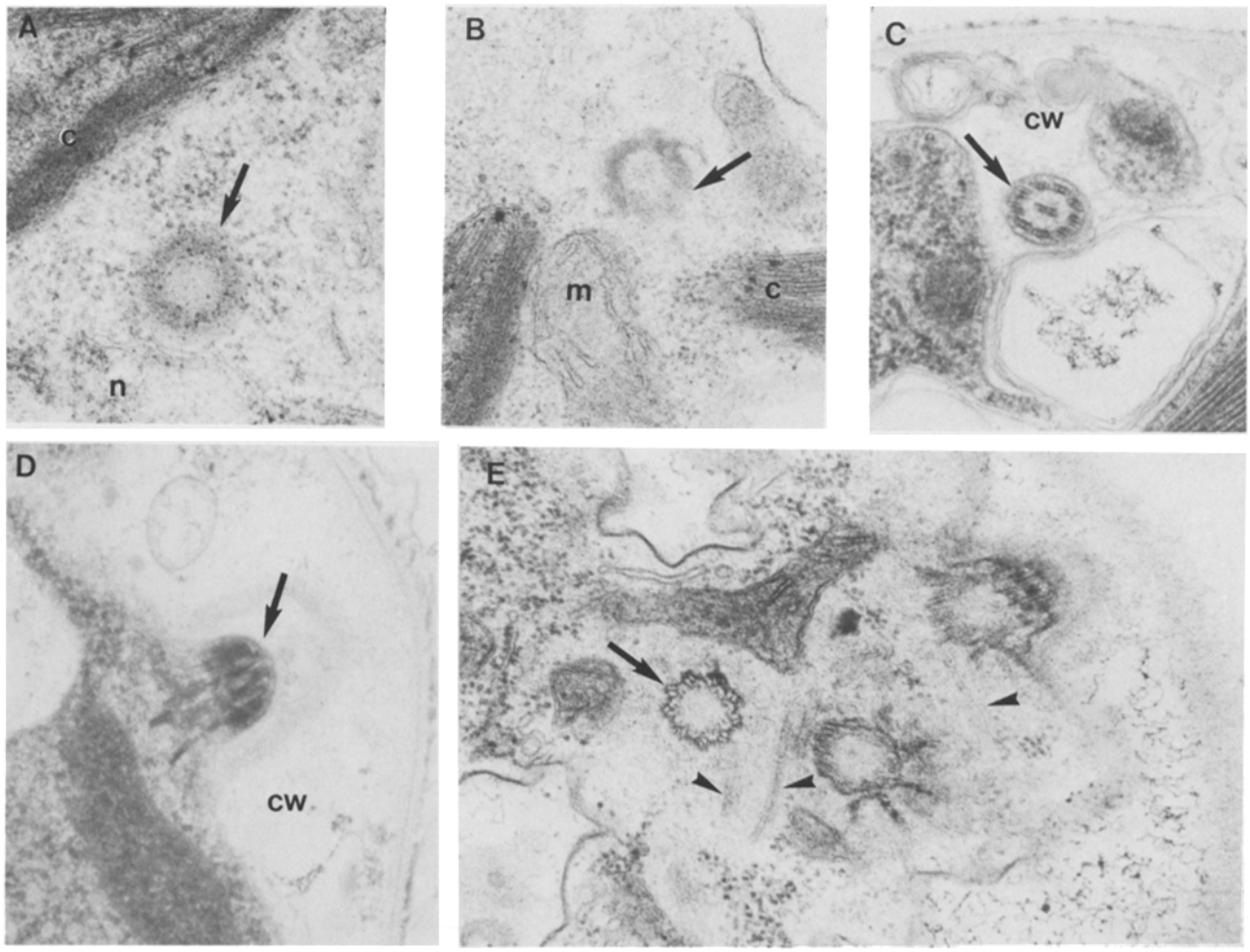

FIGURE 8 Ultrastructural abnormalities consistent with assembly of basal bodies and flagella in *vfl-1* cells during G_1. (*A* and *B*) Electron-dense rings such as these are common in *vfl-1* cells. The ring in *A* appears completely amorphous, whereas that in *B* shows some substructure of microtubule-like dimensions. (*C* and *D*) Absence of tunnels through the cell wall. (*C*) Cross-sectioned axoneme present in the cell wall without a tunnel. Such arrangements have never been observed in wild-type. × 44,200. (*D*) The membrane is intact over the transition region of this basal body. × 48,600. (*E*) Large arrow points to a basal body with doublet rather than triplet microtubules. The position of the structure in the cytoplasm, the absence of a central pair of microtubules, and the tilt of the doublets mark this structure as a basal body rather than an axoneme. × 49,500. *c*, chloroplast; *cw*, cell wall; *n*, nucleus.

connected two basal bodies, but even then the angle between the basal bodies was abnormally large or small.

Cytoplasmic microtubules were present in some *vfl-1* sections, but they were not nearly as frequent as in wild type, and the normal cruciate convergence of rootlet microtubules at the basal body complex was never observed. In addition, microtubule ultrastructure was not well resolved. Because so few sections showed cytoplasmic microtubules, we do not know whether this observation is significant; perhaps the *vfl-1* microtubules are structurally or chemically different from those in wild type, but perhaps we simply didn't observe enough examples to find good clean sections. In either case, we conclude that *vfl-1* has an incomplete and misarranged microtubular cytoskeleton.

Genetic Analysis

Tetrad analysis (Table V) indicated that the *vfl-1* mutation segregates in a Mendelian manner and that it is approximately 23 map units from *pf-3* and 10 map units from *ac-157*. *pf-3* is about 30 map units from the centromere on the left arm of Chromosome VIII and *ac-157* is 6 map units from the centromere on the right arm; thus *vfl-1* is near the centromere of Chromosome VIII, most likely on the left arm. Tetrad data with respect to the Chromosome III centromere marker *ac-17* confirm the centromere linkage and give a *vfl-1*-to-centromere distance of 4 map units. Dominance tests showed that the *vfl-1* mutation is recessive to wild type, in that *vfl-1/wild type* vegetative diploid cells were biflagellate like *wild type/wild type* diploids.

DISCUSSION

Defective Basal Body Cycle in vfl-1

In wild-type *Chlamydomonas*, the assembly of new flagella is confined to a short interval in the cell cycle (2). As mitosis approaches, the cell resorbs its flagella and then remains flagella-less throughout mitosis and cytokinesis (2, 12). After cell division is completed, each daughter cell assembles and

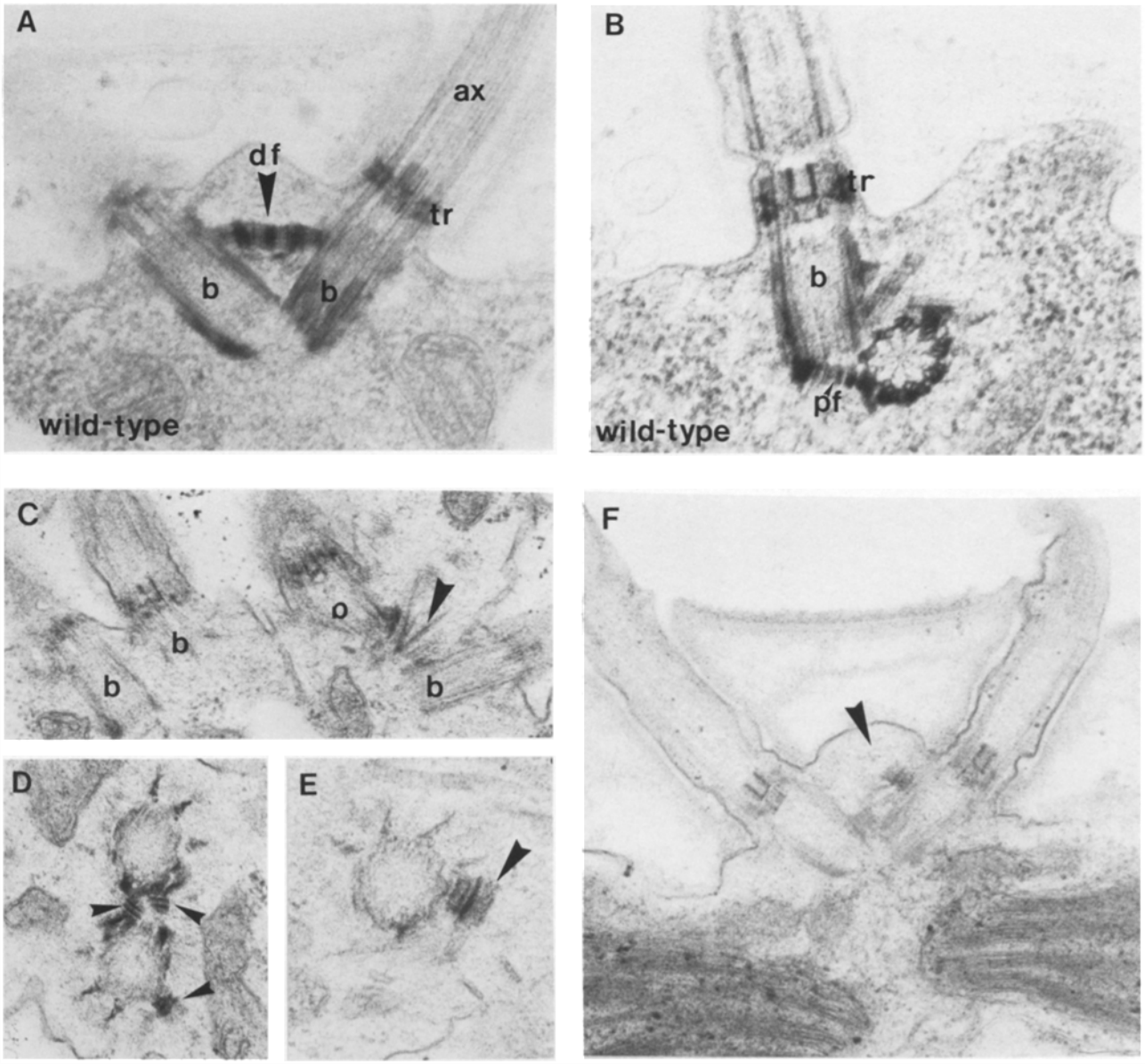

FIGURE 9 Abnormal striated fibers and microtubule rootlets in *vfl-1*. (*A* and *B*) Organization of basal bodies and striated fibers in wild type. In *A*, the 90° angle between basal bodies and the distal fiber connection are apparent. × 55,700. *B* presents a different plane of section demonstrating the proximal fiber connections at the cytoplasmic end of the basal bodies. × 56,900. (*C–F*) Abnormal striated fibers in *vfl-1*. (*C*) Four basal bodies are present in longitudinal section; no distal fiber connections are present (they should be visible in this plane of section, if present). The arrow marks an unusual structure between two of the basal bodies. × 35,900. (*D*) Three fibrous structures (arrows) are present on the cross-sectioned basal bodies. The wedge shape is typical of proximal fibers, but, in wild type, these would never be present at the same level as transitional fibers. × 34,900. (*E*) An apparently half-length distal fiber is associated with the basal body in this section. × 55,000 (*F*) The basal bodies here are in a normal position (see Fig. 9*A*) but no distal fiber spans the space between them. A short, distal fiber-like structure is present on one basal body, in the appropriate position. × 37,100. *ax*, axoneme; *b*, basal body; *df*, distal fiber; *pf*, proximal fiber; *tr*, transition region between basal body and axoneme.

maintains two flagella until the next mitosis, whereupon the cycle begins again. The cycle of flagellar assembly described above reflects and is dependent upon an underlying cycle of basal body assembly, maturation, and segregation. Early in G_1 two probasal bodies appear adjacent to the two mature axoneme-bearing basal bodies. By late G_1 these probasal bodies have matured into ultrastructurally complete basal bodies (2, 8). These newly matured basal bodies are not yet competent to assemble flagella, since the cells remain biflagellate and regenerate only two flagella following deflagellation although four basal bodies are present in the cytoplasm. During mitosis, the basal bodies, now without axonemes, can be observed in pairs near the spindle poles (3). It is probable that basal body segregation at cytokinesis is semiconservative; if so, each basal body pair consists of one newly matured and one experienced (i.e., previously flagellated) basal body (11). Frequently, daughter cells immediately undergo one or two further rounds of mitosis before flagellar assembly is initiated (4); the pattern of basal body biogenesis and segregation in these cases is unknown.

TABLE V
Tetrad Analysis

Markers scored	PD	NPD	T	Map distance
vfl-1, pf-3	20	0	17	23
vfl-1, ac157	24	0	6	10
vfl-1, ac17	27	19	4	4 (vfl-1 to centromere)

Results presented in this paper demonstrate that in *vfl-1* flagellar assembly is not tightly coupled to the cell cycle as it is in wild type. Instead of assembling flagella only during a narrow, well-defined "window" at the beginning of G_1, *vfl-1* cells assemble new flagella throughout G_1. Observations of cell populations and of individual immobilized cells indicate that flagella are added randomly at a rate of about 0.05 flagella per cell per hour.

Electron microscopic results suggest that the defect in the flagellar assembly cycle reflects an underlying defect in the basal body cycle such that basal body synthesis occurs throughout G_1. In particular, we have observed objects in *vfl-1* cells that appear to be intermediates in basal body assembly. These include basal bodies composed of doublet rather than triplet microtubules and electron-dense rings of approximate basal body diameter. The latter resemble the "amorphous discs" observed by Cavalier-Smith (2) in early-G_1 cells at sites where probasal bodies would later appear. Neither doublet-containing basal bodies nor electron-dense rings were seen in wild-type controls or in the other *vfl* mutants examined. Of course, it is possible that the objects that appear to be early intermediates in basal body assembly are something else entirely. Perhaps the increase in flagellar number observed during interphase reflects the completion of late stages in basal body maturation—that is, the conversion of basal bodies that appear ultrastructurally complete but are unable to nucleate axoneme formation into fully mature basal bodies that are capable of initiating axoneme assembly. Even if the production of additional flagella on *vfl-1* cells is due to maturation of basal bodies already present in the cytoplasm, rather than to the initiation and completion of new basal assembly, *vfl-1* can still be properly said to be defective in the temporal control of the basal body cycle, though in a different and rather more limited sense than implied previously.

Empty tunnels through the cell wall were not observed in *vfl-1* sections, which suggests that flagella formation and tunnel formation may be concurrent. It seems reasonable that, as Cavalier-Smith suggested (2), the flagella themselves could serve as templates for tunnel formation or even actively participate in the process. In any case, the existence or formation of a tunnel is not a limiting factor for the addition of flagella on *vfl-1* cells since a *vfl-1*, *cw-15* double mutant displays a flagellar number distribution similar to that of its walled *vfl* parent (data not shown). If tunnel formation were limiting, we would expect a shift in the flagellar number distribution toward a larger mean number of flagella per cell.

Defective Cytokinesis and Organelle Placement in vfl-1

Organelles are often misplaced in *vfl-1*, and cytokinesis frequently fails to partition the cell evenly in two. Basal body–associated striated fibers are absent or incomplete, and rootlet microtubules are typically misplaced. Another *vfl* mutant, *vfl-3*, shows a similar phenotype (17). It is not known how organelle or cleavage furrow localization is achieved, and so it is not possible to interpret these defects in molecular terms. Two contrasting possibilities are worth mentioning, however. One is that the basal bodies themselves play important roles in organizing the cytoplasm so that other organelles are properly placed and so that the cleavage furrow passes cleanly between basal body pairs and daughter nuclei. If this were the case, then the presence of basal bodies at abnormal locations in *vfl-1* and *vfl-3* might lead directly to misplaced organelles and misplaced cleavage furrows. Such organizing functions might be mediated by the rootlet microtubules that radiate into the cytoplasm from the region beneath the distal striated fiber and/or by the numerous microtubules that radiate from the basal body region at cytokinesis and line the cleavage furrow (12). Alternatively, the abnormalities in basal body placement and number might derive from defects in an as-yet-unidentified cytoplasmic organizing system that is also responsible for localizing other organelles and/or the cleavage furrow. If this were the case, then the relation between the basal body defects and the other defects would not be one of cause and effect.

Aberrant Motility in vfl-1 Is Due to Abnormal Placement or Rotational Orientation of Flagella

We attribute the aberrant motility of *vfl-1* to defective flagellar location or orientation and not to defective flagellar structure per se. While flagellar location in many *vfl-1* cells is decidedly abnormal (Fig. 2), and this should be sufficient to produce aberrant motility, some cells do have closely paired anterior flagella, and it might seem that these should swim normally. However, normal motility requires that the two flagellar wave forms possess 180° rotational symmetry with respect to one another. The basal body–associated striated fibers are probably required to ensure that this symmetry exists (10, 17), and since the fibers are defective in *vfl-1*, abnormal motility in almost every *vfl-1* cell is expected. Because the defects of *vfl-1* at the basal body level are sufficient to produce the aberrant motility phenotype, there is no reason to invoke abnormalities in the flagella themselves. In fact, we have failed to note any defects in axoneme ultrastructure in *vfl-1* nor were any protein-composition abnormalities revealed by two-dimensional gel electrophoresis/autoradiography of S-35 labeled *vfl-1* flagella (data not shown).

Relation of vfl-1 to Other vfl Mutants

vfl-1 is genetically and phenotypically distinct from other *C. reinhardtii* variable flagella mutants that have been described in the literature. In phenotype it most closely resembles *vfl-3* (see previous discussion), but *vfl-3* cells do not accumulate flagella throughout G_1 as *vfl-1* cells clearly do. The *vfl-3* and *vfl-1* loci are unlinked genetically: *vfl-3* is linked to the centromere of chromosome VI (17) and *vfl-1* is on chromosome VIII, also centromere linked. Another *vfl* gene, *vfl-2* (13), has not yet been mapped to a particular chromosome, but it has been demonstrated to be unlinked to either *vfl-1* or *vfl-3* (data not shown). Furthermore, the *vfl-2* phenotype differs from that of *vfl-1* or *vfl-3* in that *vfl-2* cell size is fully normal (13). A variable flagella number mutant designated *cyt-1* was described some years ago (15). *cyt-1* cells often fail to complete cytokinesis, which leads to the generation of many large multinucleate cells with multiple pairs of flagella.

Mutants like *cyt-1* with apparent defects in cytokinesis are not particularly rare, as we have isolated several others with similar phenotypes (unpublished data). Another locus with mutations affecting flagellar number is *uni-1* (11). Most *uni-1* cells in a population carry a single flagellum. Unlike *vfl-1*, *uni-1* mutants appear to be normal with respect to basal body biogenesis and segregation.

Might vfl-1 Have a Regulatory Role?

Our results demonstrate that a recessive mutation in the Mendelian gene *vfl-1* dramatically alters the temporal and spatial control of the *Chlamydomonas* flagellar assembly cycle by affecting some aspect of the underlying basal body cycle. Since recessive phenotypes typically have a loss-of-function basis, our results may indicate the existence of a *vfl-1*-dependent function—formally regulatory in nature—which normally confines basal body biogenesis to appropriate times and places during the cell cycle.

Please address reprint requests to Dr. Wright.

Dr. Adams isolated *vfl-1* and performed initial experiments in the laboratory of David J. L. Luck. We wish to thank Dr. Luck for thought-provoking discussions.

This research was supported by National Institutes of Health (NIH) grant GM17132 to Dr. Luck, NIH Biomedical Research Support Grant 2S07RR07039-10 to Dr. Adams, and National Science Foundation Grant PCM-8216337 and NIH Research Career Development Award K04AM00710 to Dr. Jarvik.

Received for publication 15 June 1984, and in revised form 18 October 1984.

REFERENCES

1. Adams, G. M. W., B. Huang, D. J. L. Luck. 1982. Temperature sensitive, assembly defective flagella mutants of *Chlamydomonas reinhardtii*. *Genetics*. 100:579–586.
2. Cavalier-Smith, T. 1974. Basal body and flagellar development during the vegetative cell cycle and the sexual cycle of *Chlamydomonas reinhardtii*. *J. Cell Sci.* 16:529–556.
3. Coss, R. A. 1974. Mitosis in *Chlamydomonas reinhardtii* basal bodies and the mitotic apparatus. *J. Cell Biol.* 63:325–329.
4. Craigie, R. A., and T. Cavalier-Smith. 1982. Cell volume and the control of the *Chlamydomonas* cell cycle. *J. Cell Sci.* 54:173–191.
5. Ebersold, W. T. 1967. *Chlamydomonas* reinhardi: heterozygous diploid strains. *Science (Wash. DC)*. 157:447–449.
6. Ebersold, W. T., R. P. Levine, E. E. Levine, and M. A. Olmstead. 1962. Linkage maps in *Chlamydomonas reinhardtii*. *Genetics*. 47:531–543.
7. Franke, W. W., S. Krien, and R. M. Brown, Jr. 1969. Simultaneous glutaraldehyde-osmium tetroxide fixation with post osmication, an improved fixation procedure for electron microscopy of plant and animal cells. *Histochemie*. 19:162–164.
8. Gould, R. R. 1975. The basal bodies of *Chlamydomonas reinhardtii*. *J. Cell Biol.* 65:65–74.
9. Gowans, C. S. 1965. Tetrad analysis. *Taiwania*. 1:1–19.
10. Hoops, H. J., R. L. Wright, J. W. Jarvik, and G. B. Witman. 1984. Flagellar waveform and rotational orientation in a *Chlamydomonas* mutant lacking normal striated fibers. *J. Cell Biol.* 98:818–824.
11. Huang, B., Z. Ramanis, S. K. Dutcher, and D. J. L. Luck. 1982. Uniflagellar mutants of *Chlamydomonas*: evidence for the role of basal bodies in transmission of positional information. *Cell*. 29:745–753.
12. Johnson, U. W., and K. R. Porter. 1968. Fine structure of cell division in *Chlamydomonas reinhardtii*. *J. Cell Biol.* 38:403–425.
13. Kuchka, M. R., and J. W. Jarvik. 1982. Analysis of flagellar size control using a mutant of *Chlamydomonas reinhardtii* with a variable number of flagella. *J. Cell Biol.* 92:170–175.
14. Sager, R., and S. Granick. 1953. Nutritional Studies with *Chlamydomonas reinhardtii*. *Ann. NY Acad. Sci.* 56:831–838.
15. Warr, J. R. 1968. A mutant of *Chlamydomonas reinhardii* with abnormal cell division. *J. Gen. Microbiol.* 52:243–251.
16. Wheatley, D. N. 1982. The Centriole: A Central Enigma of Cell Biology. Elsevier Biomedical Press, Amsterdam. 147–184.
17. Wright, R. L., B. Chojnacki, and J. W. Jarvik. 1983. Abnormal basal-body number, location, and orientation in a striated fiber-defective mutant of *Chlamydomonas reinhardtii*. *J. Cell Biol.* 96:1697–1707.